Realistic Shell-Model Calculations for Nuclei in the Region of Shell Closures off Stability

A. Covello, L. Coraggio, and A. Gargano
Dipartimento di Scienze Fisiche, Università di Napoli Federico II,
and Istituto Nazionale di Fisica Nucleare,
Complesso Universitario di Monte S. Angelo, Via Cintia - 80126 Napoli, Italy
(February 9, 2008)

We have performed realistic shell-model calculations for nuclei around doubly magic ^{100}Sn and ^{132}Sn using an effective interaction derived from the Bonn A nucleon-nucleon potential. The results are in remarkably good agreement with the experimental data showing the ability of our effective interaction to provide an accurate description of nuclear structure properties.

21.60.Cs, 21.30.Fe, 27.60.+j

I. INTRODUCTION

A fundamental goal in nuclear structure theory is to understand the properties of complex nuclei in terms of the nucleon-nucleon (NN) interaction. Since the pioneering work of Kuo and Brown [1], who in the mid 1960s derived an s-d shell effective interaction from the Hamada-Johnston potential [2], there has been considerable progress in this field. On the one hand, the theoretical framework in which the model-space effective interaction $V_{\rm eff}$ can be derived from a given (NN) potential has been largely improved (the main aspects of this derivation are reviewed in Ref. [3]). On the other hand, high-quality NN potentials have been constructed which give a very good description of the NN scattering data. A comprehensive review of modern NN potentials suitable for application in nuclear structure is given in Ref. [4].

These improvements have brought about a great deal of renewed interest in realistic shell-model calculations. In this context, the main question is to which extent modern realistic interactions can provide a consistent and accurate description of nuclear structure phenomena. To try to answer this question, the study of nuclei in the vicinity of closed shell is extremely important. In fact, they provide the best testing ground for the basic ingredients of a shell-model calculation, in particular as regards the matrix elements of the effective NN interaction.

In this paper, we shall present some results of realistic shell-model calculations for nuclei around doubly magic ^{100}Sn and ^{132}Sn. They are the $N = 50$ isotones ^{98}Cd, ^{97}Ag, ^{96}Pd, the $N = 82$ isotones ^{134}Te and ^{135}I, and the doubly odd nucleus ^{132}Sb, which has a single proton outside the $Z = 50$ closed shell and a single neutron hole in the closed $N = 82$ shell. These nuclei lie well away from the valley of stability and only recently more experimental information has become available which is of great value for a stringent test of our calculated effective interaction. It should be noted that the study of ^{132}Sb provides a direct test of the effective interaction matrix elements with isospin $T = 0$.

In earlier works we have performed shell-model calculations for the light Sn isotopes making use of two effective interactions derived from different free NN potentials. They are the Paris [5] and Bonn A [6] potentials. It turned out that the latter, which has a weaker tensor force component, leads to the best agreement with experiment for all of the nuclei considered [7,8]. For this reason, we have used it in the present work.

Our presentation is organized as follows. In Sect. 2 we give a brief description of our calculations. In Sect. 3 we present our results and compare them with the experimental data. Sect. 4 presents a summary of our conclusions.

II. OUTLINE OF CALCULATIONS

As already mentioned in the Introduction, we make use of a two-body effective interaction derived from the meson theoretic Bonn A potential. This was obtained using a G-matrix folded-diagram formalism, including renormalizations from both core polarization and folded diagrams. A description of the derivation of the effective interaction $V_{\rm eff}$ from the nucleon-nucleon potential including references can be found in Ref. [3]. We only outline here the essential of the method and point out the main differences between our present and earlier calculations [7–9].

The effective interaction can be schematically written [10] in operator form as

$$V_{\rm eff} = \hat{Q} - \hat{Q}' \int \hat{Q} + \hat{Q}' \int \hat{Q} \int \hat{Q} - \hat{Q}' \int \hat{Q} \int \hat{Q} \int \hat{Q} \cdots , \tag{1}$$

where $\hat{Q}$ and $\hat{Q}'$ represent the $\hat{Q}$-box, composed of irreducible valence-linked diagrams, and the integral sign represents a generalized folding operation. We take the $\hat{Q}$-box to be composed of G-matrix diagrams through second-order in G; they are just the seven first- and second-order diagrams considered by Shurpin *et al.* [11]. To calculate the effective interaction $V_{\rm eff}$ given by Eq. (1), a first step is to calculate the irreducible $\hat{Q}$-box diagrams and their energy derivatives in terms of the model-space G-matrix defined by [12]

$$G(\omega) = V + VQ_2 \frac{1}{\omega - Q_2 T Q_2} Q_2 G(\omega). \tag{2}$$

Here Q_2 is the Pauli exclusion operator for the two interacting nucleons, V represents the NN potential, T denotes the two-nucleon kinetic energy, and ω is the so-called starting energy. We employ a matrix inversion method to calculate the above G matrix in an essentially exact way [12].

For the $N = 50$ isotones, we have considered the doubly closed ^{100}Sn as an inert core and treated protons as valence holes. This leads to a calculation of the $\hat{Q}$-diagrams which is different from the usual one for particles. A detailed description of the calculation of our two-hole effective interaction will be given in a forthcoming publication. We have chosen the Pauli exclusion operator Q_2 in the G-matrix equation (2) as specified [12] by $(n_1, n_2, n_3) = (11, 21, 45)$. For the shell-model oscillator parameter $\hbar\omega$ we have used the value 8.5 MeV, as obtained from the expression $\hbar\omega = 45A^{-1/3} - 25A^{-2/3}$ for $A = 100$.

For the $N = 82$ isotones the valence-proton and -neutron orbits outside the ^{132}Sn core are different. Therefore, we have chosen $(n_1, n_2, n_3) = (16, 28, 55)$ for the neutron orbits and $(n_1, n_2, n_3) = (11, 21, 55)$ for the proton orbits. The effective interaction has been calculated using an isospin uncoupled representation, where neutrons and protons are treated separately. The adopted value of oscillator spacing is $\hbar\omega = 7.88$ MeV. It should be mentioned here that in our earlier study [9] we made the choice $(n_1, n_2, n_3) = (11, 28, 45)$ for both protons and neutrons. As a consequence, the Pauli exclusion operator was not treated in a completely correct way.

As regards ^{132}Sb, we have treated the odd proton and the remaining 31 neutrons as valence particles. This makes the $T = 1$ matrix elements of the effective interaction be just the same as those used in our earlier study of the Sn isotopes [7], to which we refer the reader for details.

For the $N = 82$ isotones and for ^{132}Sb our model space includes the five single-particle (s.p.) orbits $0g_{7/2}$, $1d_{5/2}$, $2s_{1/2}$, $1d_{3/2}$, and $0h_{11/2}$, while for the $N = 50$ isotones the proton holes are distributed in $0g_{9/2}$, $1p_{1/2}$, $1p_{3/2}$, and $0_{5/2}$ orbits.

As regards the choice of the s.p. energies, we have proceeded as follows. For the $N = 82$ isotones we have taken three s.p. spacings from the experimental spectrum of ^{133}Sb [13,14]. In fact, the $g_{7/2}$, $d_{5/2}$, $d_{3/2}$ and $h_{11/2}$ states can be associated with the ground state and the 0.962, 2.439 and 2.793 MeV excited levels, respectively. It should be noted that the position of the $d_{3/2}$ state corresponds to the new value very recently provided by the high-sensitivity γ spectroscopic measurement of Ref. [14]. This is about 400 keV smaller than the previously accepted value (2.708 MeV) [13]. It turns out, however, that this change has little effect on the spectra of ^{134}Te and ^{135}I. As for the $s_{1/2}$ state, its position has been determined by reproducing the experimental energy of the $\frac{1}{2}^+$ level at 2.150 MeV in ^{137}Cs. This yields the value $\epsilon_{s_{1/2}} = 2.8$ MeV.

For the $N = 50$ isotones, the single-hole energies cannot be taken from experiment, since the single-hole valence nucleus ^{99}In has not yet been studied. Therefore we have determined them from an analysis of the low-energy spectra of the isotones with $A \geq 92$. The adopted values (in MeV) are: $\epsilon_{g_{9/2}} = 0.0$, $\epsilon_{p_{1/2}} = 0.73$, $\epsilon_{p_{3/2}} = 2.17$, $\epsilon_{f_{5/2}} = 3.24$.

Regarding ^{132}Sb, we have assumed the s.p. energies to be the same for neutrons and protons. Our adopted values (in MeV) are: $\epsilon_{d_{5/2}} = 0$, $\epsilon_{g_{7/2}} = 0.20$, $\epsilon_{s_{1/2}} = 1.72$, $\epsilon_{d_{3/2}} = 1.88$, and $\epsilon_{h_{11/2}} = 2.70$. As compared to the set of s.p. energies used for the Sn isotopes (see Ref. [7]), only $\epsilon_{s_{1/2}}$ and $\epsilon_{d_{3/2}}$ have been modified. More precisely, they have been both decreased by about 0.5 MeV. It should be noted that the position of these two levels plays a minor role in the calculations for the light Sn isotopes while it is very important to satisfactorily reproduce the experimental 1_2^+ state and to place in the right energy range the calculated negative-parity states.

III. RESULTS

A. $N = 50$ isotones

In Fig. 1 we compare the calculated 2^+, 4^+, 6^+ and 8^+ yrast states of ^{98}Cd with those recently identified in the study of Ref. [15]. We see that our results are in very good agreement with experiment. A measure of the quality of the agreement between theory and experiment is given by the rms deviation σ [16], whose value is 105 keV.

It should be noted that the predicted position of the 5^- state (2.73 MeV) is quite consistent with the experimental information available for the two lighter even isotones. In fact, in ^{96}Pd and ^{94}Ru a 5^- state has been observed [17,18] at 2.648 and 2.625 MeV, respectively. As regards the structure of the excited states, we find that the positive-parity states are of practically pure $(\pi g_{9/2})^{-2}$ character while the 5^- state is dominated by the $\pi g_{9/2}^{-1} p_{1/2}^{-1}$ configuration. On the contrary, the ground-state has a significantly mixed wave function, the percentage of configurations other than $(\pi g_{9/2})^{-2}$ being about 17%.

In Figs. 2 and 3 the calculated spectra of ^{97}Ag and ^{96}Pd are compared with the experimental ones [19,17]. We see that for both nuclei our calculations produce a spectrum very close to the experimental one. The main points of disagreement are the position of the $\frac{13}{2}^+$ state in ^{97}Ag and that of the 2^+ state in ^{96}Pd which lie 213 and 281 keV, respectively, above the observed ones. The σ value is 121 keV and 130 keV for ^{97}Ag and ^{96}Pd, respectively.

Experimental information on electromagnetic transition rates in heavy $N = 50$ isotones is very scanty. It is of interest to mention here, however, that in the work of Ref. [15] a value of $0.44^{+0.20}_{-0.10}$ W.u. for the $B(E2; 8^+ \rightarrow 6^+)$ in ^{98}Cd has been reported. Using the bare proton charge $e_p = 1$ we obtain 0.67 W.u. By contrast, to reproduce the experimental value of the same $B(E2)$ in ^{96}Pd (0.34 ± 0.05 W.u.) an effective charge of at least $1.7e$ is needed. To clear up this point more experimental data are required.

B. ^{134}Te and ^{135}I

The experimental [20,21] and theoretical spectra of the two-proton nucleus ^{134}Te are compared in Fig. 4, where all the calculated and experimental levels up to 3.2 MeV excitation energy are reported. We see that while the theory reproduces all the observed levels it also predicts the existence of a 3^+ and a 0^+ state at 2.65 and 2.78 MeV, respectively. This prediction is strongly supported by the experimental information available for the two heavier even isotones. In fact, in ^{136}Xe a 0^+ state has been observed [22] at 2.58 MeV while in ^{138}Ba both a 0^+ and a 3^+ state have been located [23] at 2.34 and 2.45 MeV , respectively. Above 3.2 MeV excitation energy the comparison between theory and experiment is made only for those observed levels which have received a spin-parity assignment. We do not include the new levels observed in [24] since all of them should be interpreted as neutron particle-hole states. This interpretation is confirmed by our calculations. In fact, the only two states, having $J^\pi = 8^+$ and 10^+, which can be constructed in our model space are both predicted to lie at about 7.3 MeV while the two experimental states with these spin-parity assignments have been located [24] at 4.557 and 5.622 MeV, respectively. We see that the calculated spectrum reproduces very well the experimental one, the discrepancies between theory and experiment being smaller than 50 keV for several states (9 out of 15). The rms deviation σ is 106 keV.

In Fig. 5 we compare the calculated spectrum of ^{135}I with the experimental one [24,25] up to 4.0 MeV excitation energy. As in the case of ^{134}Te, we exclude the experimental levels above 4.2 MeV, which originate from core excitations. We should note that the spectra of Fig. 5 include all experimental and calculated levels up to 1.5 MeV. Above this energy several other levels without assigned spin and parity are reported in [25]; we compare our calculated states only with those observed in [24]. From Fig. 5 we see that the excitation energies are remarkably well reproduced for all the reported states, the σ value being 58 keV. We have associated the experimental level at 1.010 MeV with the theoretical $\frac{3}{2}^+$ at 0.931 MeV.

We should now point out that the theoretical results presented here for ^{134}Te and ^{135}I are in a substantially better agreement with experiment than those obtained in our earlier study [9]. The reason for these improvements can be clearly traced to the better treatment of the Pauli exclusion operator Q_2.

In Table I we compare the experimental reduced transition probabilities in ^{134}Te with the calculated ones. We have used an effective proton charge $e_p^{\rm eff} = 1.55e$. This is consistent with the values adopted by other authors [26,27]. The theoretical $B(E2)$ values are in very good agreement with experiment. As regards the $E3$ transitions, we find that the $B(E3; 9_1^- \rightarrow 6_2^+)$ is well reproduced while the $B(E3; 9_1^- \rightarrow 6_1^+)$ is underestimated by a factor of about 4. A possible reason for this discrepancy lies in the fact that only a small amount of configuration mixing is present in the calculated 6^+ states. In fact, the decay to the 6_2^+ state is dominated by the single-proton transition $(h_{11/2} g_{7/2})_{9^-} \rightarrow (g_{7/2} d_{5/2})_{6^+}$ while that to the 6_1^+ state by the transition $(h_{11/2} g_{7/2})_{9^-} \rightarrow (g_{7/2}^2)_{6^+}$, which is retarded owing to spin flip. The theoretical $B(E3; 9_1^- \rightarrow 6_1^+)$ value could be brought in agreement with experiment by an amount of configuration mixing of about 15%, which would, of course, reduce the $B(E3; 9_1^- \rightarrow 6_2^+)$ value. It should be noted, however, that the latter would still be within the error bar.

C. ^{132}Sb

The experimental and theoretical spectra of ^{132}Sb are compared in Fig. 6, where all the observed levels are reported. In the calculated spectrum all levels up to 1.4 MeV excitation energy are included while in the higher energy region only the 1_2^+ and 3_2^- states are reported. It should be noted that the nature of the presently available experimental information is quite different for positive- and negative-parity levels. In fact, while the spin-parity assignments to the former have been clarified by the study of Ref. [28], this is not the case for the latter. More precisely, the excitation energy of the 8^- state is not known (the work of Ref. [29] places it between 150 and 250 keV) and the three other observed negative-parity states have not received firm spin assignments. We find that the first excited 8^- state lies at 126 keV while the 6_1^-, 5_1^-, 7_1^-, 3_1^-, and 4_1^- states are grouped in a very small energy interval (from 210 to 380 keV). As a consequence, any attempt to establish a one-to-one correspondence between the observed levels and those predicted by our calculation could be misleading. It is of interest to note that the above states, which all arise from the $\pi g_{7/2}\nu h_{11/2}$ configuration, are well separated from the other two members of the multiplet, i.e. the 9^- and 2^- states, which are predicted at 1.0 and 1.42 MeV, respectively. A similar behavior is also predicted for the $\pi d_{5/2}\nu h_{11/2}^{-1}$ multiplet. In fact, the 7^-, 6^-, 5^-, and 4^- states belonging to this configuration lie between 0.82 and 0.97 Mev while the highest- and lowest-spin members (8^- and 3^-) are at 1.12 and 1.56 MeV, respectively.

From Fig. 6 we see that the experimental excitation energies of the positive-parity states are remarkably well reproduced by the theory, the largest discrepancy being 77 keV for the 5_1^+ state. The value of the rms deviation σ is only 32 keV.

In Table II we compare the $BE(2)$ values for transitions between states below 1.1 MeV excitation energy with the calculated ones. A more complete analysis of the electromagnetic properties of ^{132}Sb may be found in [30]. We have used an effective proton charge $e_p^{\rm eff} = 1.55e$, which is just the same as that adopted for the $N = 82$ isotones. No effective charge has been attributed to the neutron hole. As we see from Table II, the experimental data are affected by large errors. In view of this, the agreement between theory and experiment can be considered quite satisfactory. In fact, our calculated values lie all but two within the limits set by experiment.

IV. CONCLUDING REMARKS

We have presented here some recent results of realistic shell-model calculations for nuclei around doubly magic ^{100}Sn and ^{132}Sn. They have been obtained by employing an effective interaction derived from the Bonn A nucleon-nucleon potential. We have shown that the agreement between theory and experiment is very good for all nuclei considered. It is to be emphasized that the study of ^{132}Sb provides a test of our $T = 0$ effective interaction in this mass region. This is of special interest since in earlier works using different NN potentials it turned out that not enough attraction was provided by the calculated matrix elements of the $T = 0$ effective interaction, which has a stronger dependence on the tensor force strength than the $T = 1$ interaction (a detailed discussion of this important point including references is given in Ref. [31]).

In conclusion, the success achieved by our calculations shows that our effective interaction derived from the Bonn A NN potential is able to describe with quantitative accuracy the spectroscopic properties of nuclei near closed shells.

ACKNOWLEDGMENTS

The results presented in this paper are part of a research program carried out in collaboration with F. Andreozzi, T. T. S. Kuo, and A. Porrino. This work was supported in part by the Italian Ministero dell'Università e della Ricerca Scientifica e Tecnologica (MURST).

[1] Kuo T. T. S. and Brown G. E., Nucl. Phys. **85** (1966) 40.
[2] Hamada T. and Johnston I. D., Nucl. Phys. **34** (1962) 382.
[3] Kuo T. T. S., in *New Perspectives in Nuclear Structure (Ravello 1995)*, edited by A. Covello (World Scientific, Singapore, 1996), p. 159.
[4] Machleidt R. and Li G. Q., Phys. Rep. **242** (1994) 5.

[5] Lacombe M., Loiseau B., Richard J. M., Vinh Mau R., Côté J., Pirès P. and de Tourreil R., Phys. Rev. C **21** (1980) 861.
[6] Machleidt R., Holinde K. and Elster Ch., Phys. Rep. **149** (1987) 1.
[7] Andreozzi F., Coraggio L., Covello A., Gargano A., Kuo T. T. S., Li Z. B. and Porrino A., Phys. Rev. C **54** (1996) 1636.
[8] Covello A., Andreozzi F., Coraggio L., Gargano A., Kuo T. T. S. and Porrino A., Prog. Part. Nucl. Phys. **38** (1997) 165.
[9] Andreozzi F., Coraggio L., Covello A., Gargano A., Kuo T. T. S. and Porrino A., Phys. Rev. C **56** (1997) R16.
[10] Kuo T. T. S and Osnes E., *Lecture Notes in Physics*, Vol. 364 (Springer-Verlag, Berlin, 1990).
[11] Shurpin J., Strottman D. and Kuo T. T. S., Nucl. Phys. A **408** (1983) 310.
[12] Krenciglowa E. M., Kung C. L., Kuo T. T. S. and Osnes E., Ann. Phys. (N.Y.) **101** (1976) 154.
[13] Sergenkov Yu. V. and Sigalov V. M., Nucl. Data Sheets **49** (1986) 39.
[14] Sanchez Vega M. *et al.*, Phys. Rev. Lett., in press.
[15] Górska M. *et al.*, Phys. Rev. Lett. **79** (1997) 2415.
[16] We define $\sigma = \{\frac{1}{N_d}\sum_i [E_{\rm exp}(i) - E_{\rm calc}(i)]^2\}^{1/2}$, where N_d is the number of data.
[17] Peker L. K., Nucl. Data Sheets **68** (1993) 165.
[18] Tuli J. K., Nucl. Data Sheets **66** (1992) 1.
[19] Artna-Cohen Agda, Nucl. Data Sheets **70** (1993) 85.
[20] Omtvedt J. P., Mach H., Fogelberg B., Jerrestam D., Hellström M., Spanier L., Erokhina K. I. and Isakov V. I., Phys. Rev. Lett. **75**, (1995) 3090.
[21] Sergeenkov Yu. V., Nucl. Data Sheets **71**, (1994) 557.
[22] Tuli J. K., Nucl. Data Sheets **71** (1994) 1.
[23] Tuli J. K., Nucl. Data Sheets **69** (1993) 69.
[24] Zhang C. T. *et al.*, Phys. Rev. Lett. **77** (1996) 3743.
[25] Sergeenkov Yu. V., Nucl. Data Sheets **52** (1987) 205.
[26] Wildenthal B. H. and Larson D., Phys. Lett. B **37** (1971) 266.
[27] Heyde K., Sau J., Henry E. A. and Meyer R. A., Phys. Rev C **25** (1982) 3193.
[28] Mach H., Jerrestam D., Fogelberg B., Hellström M., Omtvedt J. P., Erokhina K. I. and Isakov V. I., Phys. Rev. C **51** (1995) 500.
[29] Stone C. A., Faller S. H. and Walters W. B., Phys. Rev. C **39** (1989) 1963.
[30] Andreozzi F., Coraggio L., Covello A., Gargano A., Kuo T. T. S. and Porrino A., to be published.
[31] Jiang M. F., Machleidt R., Stout D. B. and Kuo T. T. S., Phys. Rev. C **46** (1992) 910.

TABLE I. Calculated and experimental $B(E\lambda)$ values (in W.u.) for ^{134}Te. The experimental data are from [20].

$J_i^\pi \to J_f^\pi$	λ	$B(E\lambda)_{\rm expt}$	$B(E\lambda)_{\rm calc}$
$4_1^+ \to 2_1^+$	2	4.3 ± 0.3	4.2
$6_1^+ \to 4_1^+$	2	2.05 ± 0.03	1.9
$9_1^- \to 6_1^+$	3	3.8 ± 0.2	1.0
$9_1^- \to 6_2^+$	3	8.0 ± 1.3	8.2

TABLE II. Calculated and experimental $B(E2)$ values (in e^2 fm^4) for ^{132}Sb. The experimental data are from [28].

$J_i^\pi \to J_f^\pi$	$B(E2)_{\rm expt}$	$B(E2)_{\rm calc}$
$3_1^+ \to 4_1^+$	36±11	42
$2_1^+ \to 3_1^+$	76±76	53
$2_1^- \to 4_1^+$	< 26	5.8
$2_2^+ \to 3_2^+$	$1.1^{+15.4}_{-1.1}$	0.85
$2_2^+ \to 2_1^+$	37±30	4.4
$2_2^+ \to 3_1^+$	36±23	5.4
$2_2^+ \to 4_1^+$	8.4±4.5	9.1

FIG. 1. Experimental and calculated spectrum of ^{98}Cd.

FIG. 2. Experimental and calculated spectrum of ^{97}Ag.

FIG. 3. Experimental and calculated spectrum of ^{96}Pd.

FIG. 4. Experimental and calculated spectrum of ^{134}Te.

FIG. 5. Experimental and calculated spectrum of ^{135}I.

FIG. 6. Experimental and calculated spectrum of ^{132}Sb.

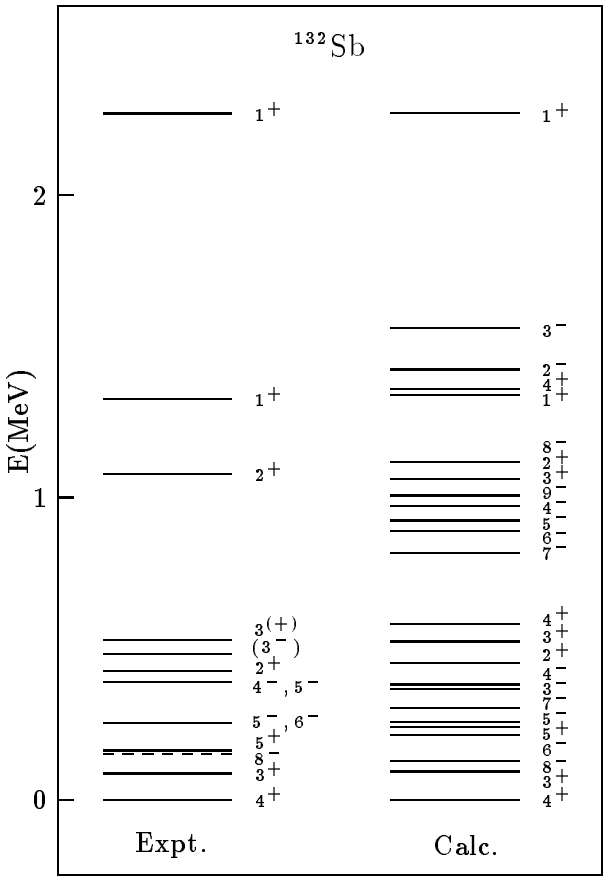
^{132}Sb
E(MeV)
2
1
0
1+
1+
2+
3(+)
(3−)
2+
4−, 5−
5−, 6−
5+
8−
3+
4+
Expt.
1+
3−
2−
4+
1+
8−
2+
3+
9−
4−
5−
6−
7−
4+
3+
2+
4−
3−
7−
5−
5+
6−
8−
3+
4+
Calc.

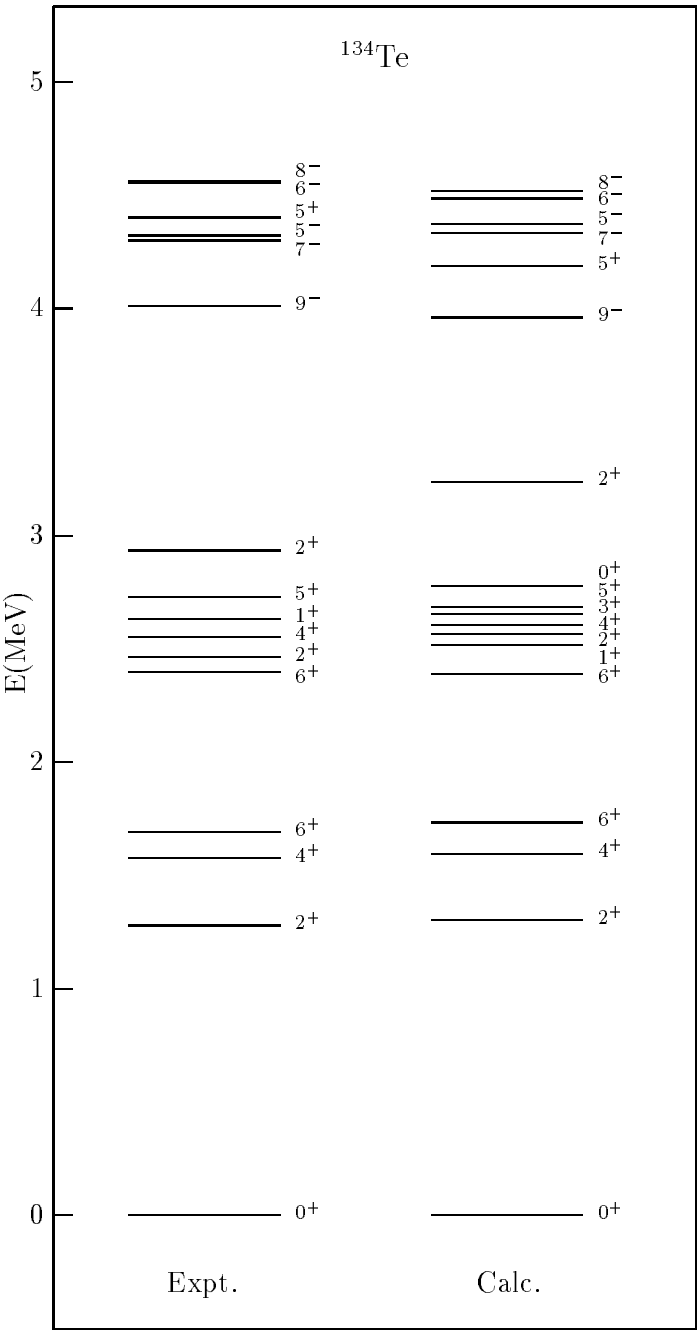
^{134}Te
E(MeV)
0
1
2
3
4
5
8^-
6^-
5^+
5^-
7^-
9^-
2^+
5^+
1^+
4^+
2^+
6^+
6^+
4^+
2^+
0^+
Expt.
8^-
6^-
5^-
7^-
5^+
9^-
2^+
0^+
5^+
3^+
4^+
2^+
1^+
6^+
6^+
4^+
2^+
0^+
Calc.

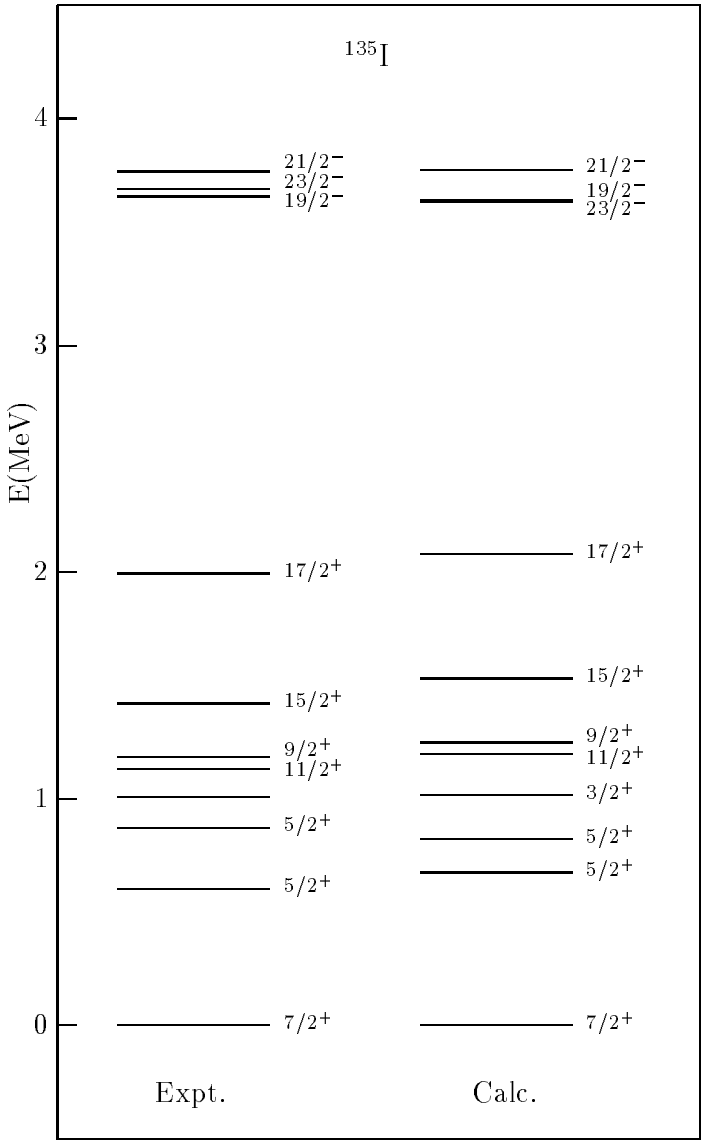
^{135}I
E(MeV)
4
3
2
1
0
$21/2^-$
$23/2^-$
$19/2^-$
$17/2^+$
$15/2^+$
$9/2^+$
$11/2^+$
$5/2^+$
$5/2^+$
$7/2^+$
$21/2^-$
$19/2^-$
$23/2^-$
$17/2^+$
$15/2^+$
$9/2^+$
$11/2^+$
$3/2^+$
$5/2^+$
$5/2^+$
$7/2^+$
Expt.
Calc.

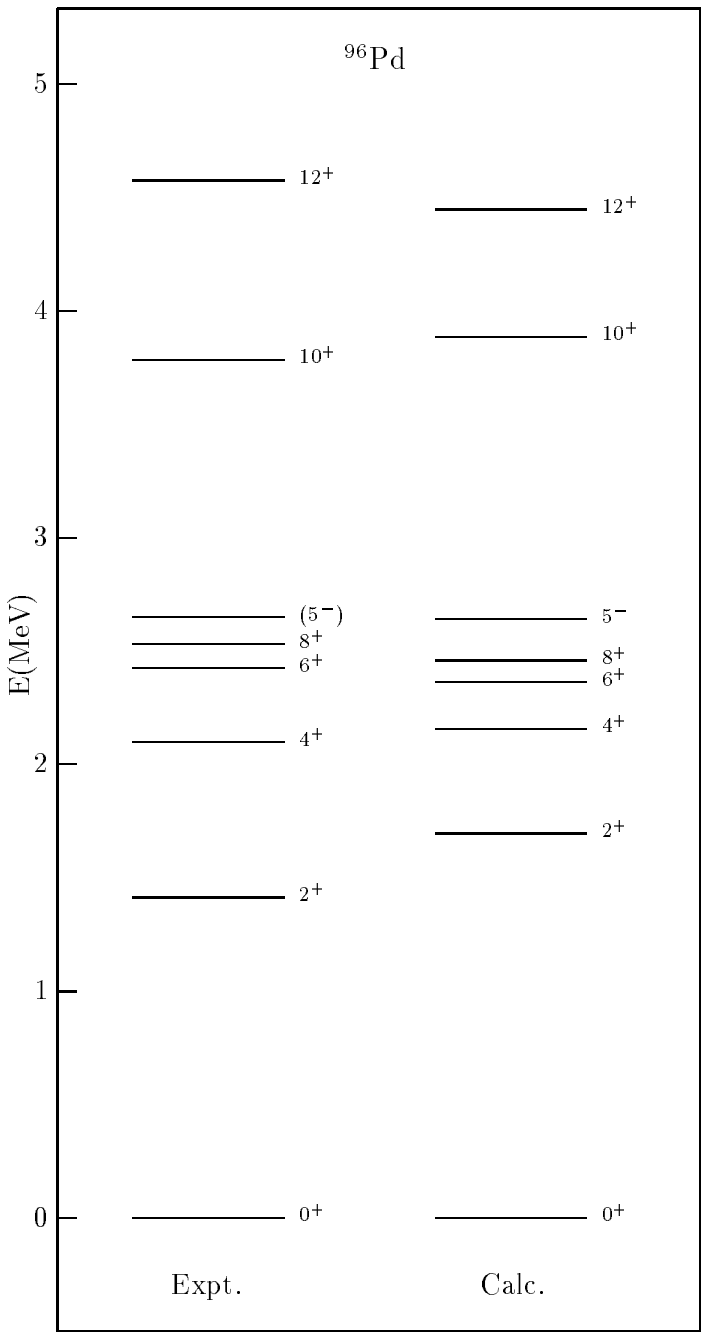
^{96}Pd
E(MeV)
5
4
3
2
1
0
12^+
10^+
(5^-)
8^+
6^+
4^+
2^+
0^+
12^+
10^+
5^-
8^+
6^+
4^+
2^+
0^+
Expt.
Calc.

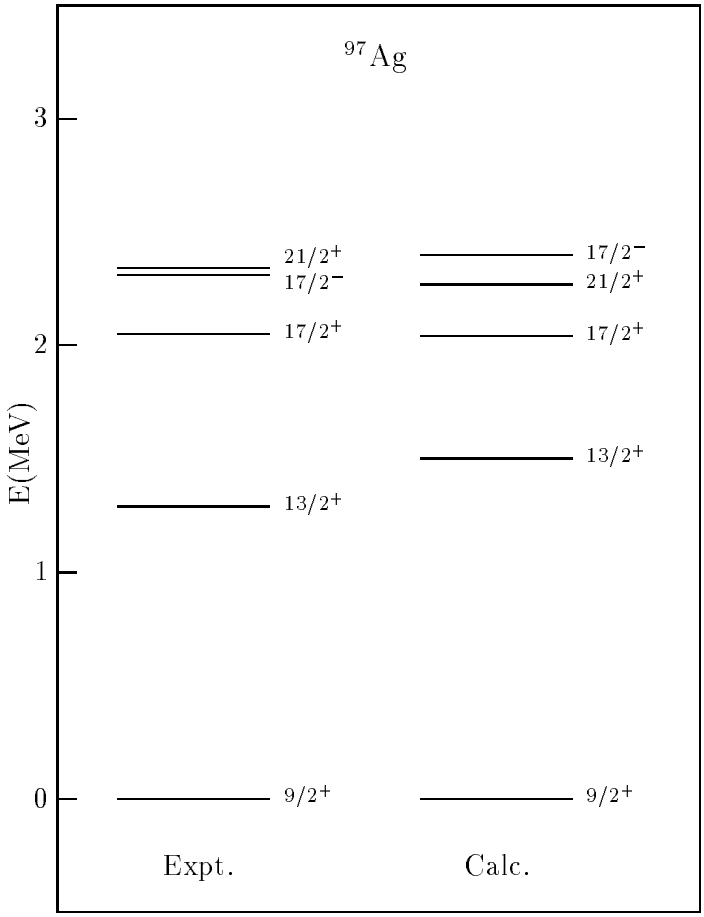
^{97}Ag
E(MeV)
3
2
1
0
$21/2^+$
$17/2^-$
$17/2^+$
$13/2^+$
$9/2^+$
$17/2^-$
$21/2^+$
$17/2^+$
$13/2^+$
$9/2^+$
Expt.
Calc.

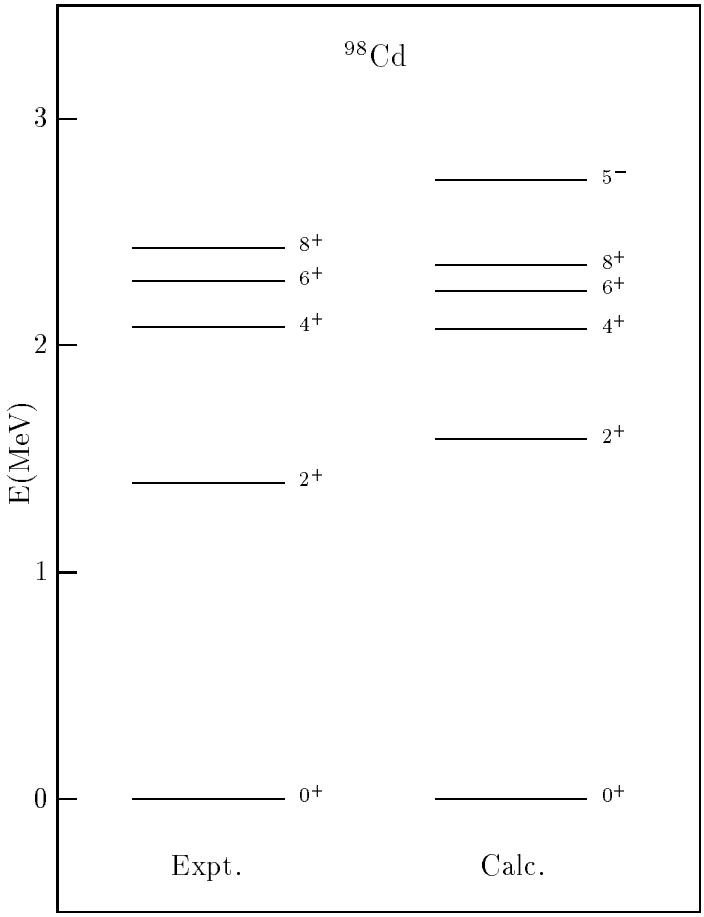
^{98}Cd
E(MeV)
3
2
1
0
8^+
6^+
4^+
2^+
0^+
5^-
8^+
6^+
4^+
2^+
0^+
Expt.
Calc.